

Experimental evidence of symmetry breaking in the multiferroic $\text{Ba}_3\text{NbFe}_3\text{Si}_2\text{O}_{14}$ using sound velocity measurements

G. Quirion,^{*} C. Bidaud, and J. A. Quilliam*Institut Quantique and Département de Physique, Université de Sherbrooke, Sherbrooke, Québec J1K 2R1, Canada*

P. Lejay, V. Simonet, and R. Ballou

Institut Néel, CNRS and Université Grenoble Alpes, 38042 Grenoble, France

(Received 18 August 2017; published 30 October 2017)

Using high-resolution sound velocity measurements, we determined the temperature dependence of the principal elastic constants of the multiferroic compound $\text{Ba}_3\text{NbFe}_3\text{Si}_2\text{O}_{14}$ at different magnetic fields. All four elastic constants revealed an anomaly at $T_N = 27.1(1)$ K, which coincides very well with the emergence of the magnetic chiral state. More importantly, we carried out velocity measurements as a function of a field rotating in the basal trigonal plane at different fields and temperatures. In particular, in the magnetically ordered state, we observed an angular hysteresis of $\Delta C_{11}/C_{11}$, which might be associated with the field-induced ferroelectric polarization suddenly switching from the b^* axis to the a direction, due to the magnetoelectric effect previously observed in $\text{Ba}_3\text{NbFe}_3\text{Si}_2\text{O}_{14}$. The data analysis also leads to an estimate for the lattice distortion ($e_1 - e_2 \leq 10^{-5}$) accounting for a symmetry reduction in the magnetic chiral state possibly associated with the induced polarization along the a axis in zero field.

DOI: [10.1103/PhysRevB.96.134433](https://doi.org/10.1103/PhysRevB.96.134433)

I. INTRODUCTION

It is now well established that antiferromagnets with triangular lattices potentially show strong magnetoelectric coupling [1–5]. Due to magnetic frustration with first neighbor antiferromagnetic interactions, these systems normally favor the in-plane 120° antiferromagnetic state which can induce an electric polarization via various mechanisms [5–8]. In some of these systems, the 120° magnetic arrangement possesses two reversed directions of rotation around the triangle, defined hereafter as triangular chirality [9]. An electric poling process is then required in order to stabilize a single chiral magnetic domain. Lately, a new approach has emerged with noncentrosymmetric langasite-type compounds [10], such as $\text{Ba}_3\text{NbFe}_3\text{Si}_2\text{O}_{14}$, where a single chiral magnetic domain is stabilized without the use of a poling process [11]. Neutron scattering measurements show that within each triangle, the Fe^{3+} magnetic moments rotate by 120° relative to each other while, at the same time, the moments form a helix with a propagation vector $q = (0, 0, \tau)$ with $\tau \approx 1/7$ [Fig. 1(b)]. Moreover, models show that the triangular chirality and the helical chirality (hereafter called helicity) along the c axis are both locked in by the structural chirality of $\text{Ba}_3\text{NbFe}_3\text{Si}_2\text{O}_{14}$ [10,12]. While the magnetic ground state of $\text{Ba}_3\text{NbFe}_3\text{Si}_2\text{O}_{14}$ is already well understood, the microscopic mechanism leading to the magnetoelectric effect in this material remains to be settled experimentally [13,14].

At ambient temperature, $\text{Ba}_3\text{NbFe}_3\text{Si}_2\text{O}_{14}$ crystallizes in the $P321$ noncentrosymmetric trigonal space group with the magnetic ion Fe^{3+} ($S = 5/2$) forming a network of isolated equilateral trimers on a two dimensional triangular lattice [Fig. 1(a)] with consecutive planes well separated by planes of oxygen ions. This particular structure leads to a complex

network of superexchange interactions between magnetic ions within each trimer, between moments on nearest trimers, and between nearest plane spins along the c axis [10,15]. This network of interaction leads to high Curie-Weiss temperature, $\theta = -174 \pm 4$ K, with a much lower Néel temperature, $T_N = 27$ K [10]. On the one hand, most neutron scattering measurements are interpreted as a dominant in-plane 120° magnetic arrangement within each trimer with a helical spin structure propagating along the c axis and $q = (0, 0, 0.1429)$ [Fig. 1(b)] [12,15]. On the other hand, new neutron results [13] seem to indicate that the relative in-plane orientation of the spins within each trimer deviates from the perfect 120° arrangement. This would imply a loss of the threefold symmetry c axis, compatible with the observation of a polarization aligned with the a axis [11,13]. However, recent infrared and Raman measurements also suggest that a ferroelectric polarization exists even above the Néel temperature T_N due to a structural phase transition ($P321 \rightarrow P1$) around $T_p \simeq 120$ K [16]. As pointed out by the authors, the main consequence of their analysis would be that $\text{Ba}_3\text{NbFe}_3\text{Si}_2\text{O}_{14}$ could no longer be considered to be a magnetically induced multiferroic. Therefore considering that a structural phase transition at $T_p \simeq 120$ K or $T_N = 27$ K has not yet been confirmed by any other experimental observations, we have undertaken a series of high resolution velocity measurements on $\text{Ba}_3\text{NbFe}_3\text{Si}_2\text{O}_{14}$ as a function of temperature and magnetic field. These measurements can also potentially shed light on the nature of the magnetoelectric effect observed in $\text{Ba}_3\text{NbFe}_3\text{Si}_2\text{O}_{14}$.

Sound velocity measurements presented in this work were realized on $\text{Ba}_3\text{NbFe}_3\text{Si}_2\text{O}_{14}$ single crystals grown by the floating zone method [17]. The samples were prepared with faces normal to $x \parallel a$, $y \parallel b^*$, and $z \parallel c$, where a and b are the trigonal lattice vectors shown in Fig. 1 and c is the trigonal axis perpendicular to the (a, b) plane. Prior to the velocity measurements, all faces were polished in order to mount two 30-MHz LiNbO_3 transverse or longitudinal piezoelectric transducers on opposite faces. An ultrasonic interferometer

^{*}Department of Physics and Physical Oceanography, Memorial University, St. John's, Newfoundland, Canada, A1B 3X7.

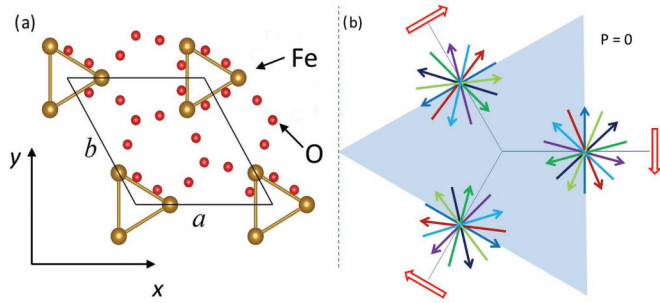


FIG. 1. (a) $\text{Ba}_3\text{NbFe}_3\text{Si}_2\text{O}_{14}$ crystal structure projected in the (a, b) plane showing the Fe^{3+} magnetic ions and the oxygen ions. (b) Spin arrangement projected in the (a, b) plane on each trimer. The same color arrows illustrate the unique chirality while the different colored arrows show the spin helicity along the c axis for seven consecutive planes. The bunching of the helices, as described in Ref. [13], leads to a net moment represented by a larger red arrow. For equilateral trimers, as shown here, no polarization would exist.

was used to measure the change in the relative velocity ($\Delta V/V$) of the first transmitted echo. The sample lengths along the directions of propagation ($1.38 \times 2.05 \times 3.88 \text{ mm}^3$) were sufficient in order to determine the relative velocity variation with a resolution better than $\Delta V/V \approx 10^{-6}$. As demonstrated over many years, this technique is well adapted to the detection of magnetic and structural phase transitions [18–22]. The velocity of longitudinal and transverse modes propagating along different directions can be used to determine the principal elastic constants [23]. For crystals with a trigonal symmetry, the specific relations between the measured velocity and the effective elastic constants C_{eff} are listed in Table I.

As determined from velocity measurements, we present in Fig. 2, the temperature dependence of the relative variation of the principal elastic constants ($\Delta C/C$) obtained for $\text{Ba}_3\text{NbFe}_3\text{Si}_2\text{O}_{14}$. All four elastic constants clearly reveal an anomaly at $T_N = 27.1(1) \text{ K}$ which coincides very well with the reported magnetic phase transition observed by magnetization and neutron scattering measurements [24]. More importantly, our results do not show any anomaly around $T_p \approx 120 \text{ K}$, recently conjectured from infrared and Raman measurements [16]. Thus, as the elastic properties are very sensitive to structural transitions, we rather believe that the symmetry of $\text{Ba}_3\text{NbFe}_3\text{Si}_2\text{O}_{14}$ remains unchanged from room temperature down to the magnetic phase transition observed at $T_N = 27.1(1) \text{ K}$.

The effect of a magnetic field on the elastic properties of $\text{Ba}_3\text{NbFe}_3\text{Si}_2\text{O}_{14}$ has also been examined. The principal

TABLE I. Effective elastic constants C_{eff} for the trigonal point group 32 for different directions of propagation and polarization relative to the cartesian coordinate axis shown in Fig. 1.

mode	Direction/polarization	$C_{\text{eff}} = \rho V^2 (10^{10} \text{ N/m}^2)$
L	[100]/[100]	$C_{11} = 12.6(3)$
L	[001]/[001]	$C_{33} = 14.8(3)$
T	[010]/[100]	$C_{66} = \frac{C_{11} - C_{12}}{2} = 3.3(1)$
T	[001]/[100]	$C_{44} = 6.2(2)$

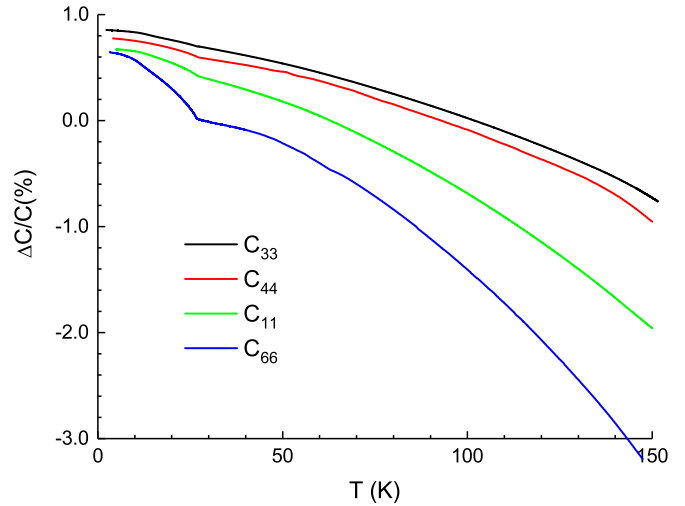


FIG. 2. Temperature dependence of the relative variation of the principal elastic constants $\Delta C/C$ of $\text{Ba}_3\text{NbFe}_3\text{Si}_2\text{O}_{14}$, C_{11} , C_{33} , C_{44} , and C_{66} .

results, for a field applied either along the c axis or the y axis, are presented in Fig. 3 and show that the Néel temperature changes at a rate of $dT_N/dH = -0.025(5) \text{ K/T}$. Moreover, the largest temperature and field variation ($\sim 0.5\%$) is observed on the shear mode ($\Delta C_{66}/C_{66}$) while the field dependence for

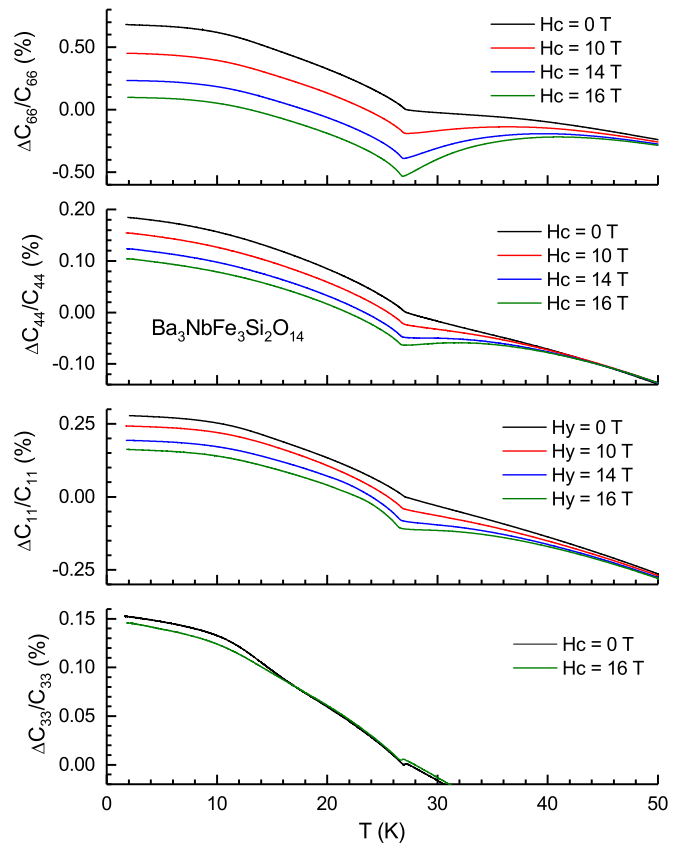


FIG. 3. Temperature dependence of the principal elastic constants measured at different magnetic fields along the c axis or the y direction.

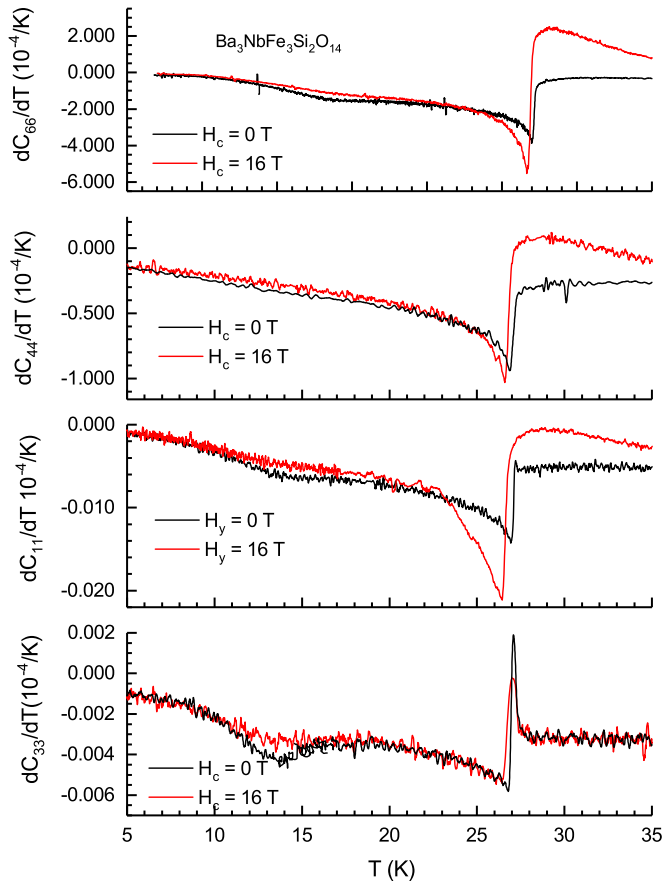


FIG. 4. Temperature derivative of the elastic constants obtained at 16 and 0 T along the c axis or the y direction.

the longitudinal mode ($\Delta C_{33}/C_{33}$) is significantly smaller. With the exception of C_{33} , all modes show field effects well above T_N which we associate with short range spin correlations clearly visible up to ~ 50 K, in agreement with neutron scattering measurements showing spin fluctuations up to 60 K [12,25]. Let add that velocity measurements as a function of a magnetic field (not shown here), for H_a and H_c , show no sign of field induced phase transitions up to 16 T at any temperatures lower than T_N .

A close inspection of $\Delta C_{33}/C_{33}$ reveals a small drop ($\sim 4 \times 10^{-5}$) at T_N (see Figs. 2 and 4). For longitudinal modes, this steplike variation is associated with linear-quadratic coupling terms ($g_i e_i S^2$) between the strain components and the order parameter [20,26]. Moreover, this coupling also accounts for the thermal lattice contraction or expansion below the Néel temperature. Therefore the step in $\Delta C_{33}/C_{33}$ is an indication that there is a lattice variation along the c axis due to the magnetic chiral order. This is supported by x-ray powder-diffraction data on the isostructural compound $\text{Ba}_3\text{SbFe}_3\text{Si}_2\text{O}_{14}$, which indeed show a small lattice expansion along the c axis [24]. Based on a Landau analysis, considering that the existence of an electric polarization along the a axis [11] can only be accounted for by a threefold symmetry breaking taking place at T_N , we would therefore expect a similar step like anomaly on C_{11} . While the absence of the steplike anomaly on C_{11} does not necessary rule out the existence of a structural transition at T_N , it is a clear indication

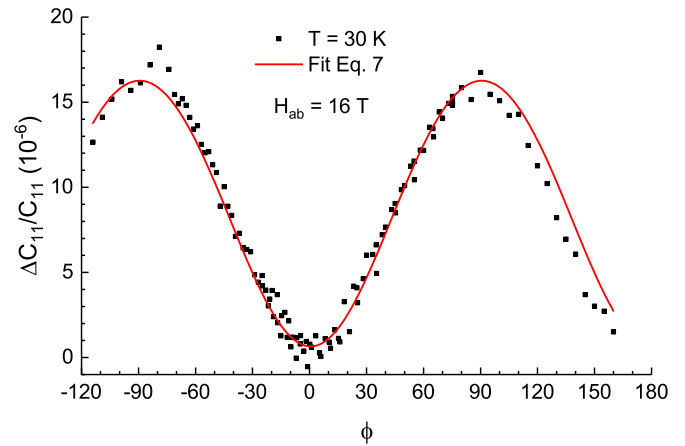


FIG. 5. Angular dependence of $\Delta C_{11}/C_{11}$ measured as a function of a field ($H = 16$ T) rotating in the ab plane in the paramagnetic state at $T = 30$ K. The continuous line is obtained using the analytical Eq. (7).

that the coupling between the electric polarization and the strain is small. This might explain why there is so far no direct evidence of a structural transition at T_N from x-ray measurements.

While the magnetic transition is clearly visible in the temperature dependence of all elastic constants, the comparison of C_{33} measured at $H_c = 0$ and 16 T reveals a second anomaly around $T_x \simeq 14$ K. In fact, a close inspection of the data presented in Fig. 4, where we present the derivative of the elastic constants (dC/dT) as a function of temperature, reveals that this anomaly is visible in all elastic constants, except for C_{44} . As the change in the slope, close to T_x , is very gradual in comparison with what we observe at T_N , we rather associate this second anomaly with a change in an electronic relaxation process, as observed in the ESR linewidth and the dielectric constant around the same temperature. [24,27,28]

Recent electric polarization measurements carried out on $\text{Ba}_3\text{NbFe}_3\text{Si}_2\text{O}_{14}$ [11] show the emergence of a dominant polarization oriented along the a axis without electric poling in zero magnetic field, which coincides with the magnetic order at T_N . Assuming that the electric polarization is related to the triangular chirality, this is in line with the fact that the complex network exchange interaction in $\text{Ba}_3\text{NbFe}_3\text{Si}_2\text{O}_{14}$ stabilizes a single chiral state below the Néel temperature, as shown by neutron scattering. These measurements also demonstrate that there is an additional electric polarization induced by a magnetic field in the triangular plane; a field applied along b^* (y) generates a polarization \vec{P}_a , while a field applied along a -axis induces a polarization \vec{P}_{b^*} . Moreover, the direction of the polarization can be reversed above a certain value of the external magnetic field. Thus, in order to gain further information about the correlation between the magnetic chiral state, the field-induced ferroelectric polarization, and the external field orientation, we measured the angular dependence of C_{11} as a function of a constant field rotating in the ab -plane. First, we present in Fig. 5 the angular dependence of $\Delta C_{11}/C_{11}$ measured in the paramagnetic state at 30 K for a field $\vec{H}_{ab} = 16$ T. The data can be analyzed using a Landau model taking into account the coupling between the strain

components and the magnetization. For a field applied in the basal plane, the total free energy can be written as

$$F_t(e_\alpha, M) = F_L(M) + F_e(e_\alpha) + F_c(e_\alpha, M). \quad (1)$$

Using the symmetry operations associated with the trigonal point group (32), the invariant terms correspond to

$$F_L(M) = \frac{A}{2}M^2 + \frac{B}{4}M^4 - \vec{M} \cdot \vec{H}, \quad (2)$$

which represents the Landau free energy expansion in terms of the induced magnetization M . The elastic energy associated with the trigonal point group (32) is given by

$$\begin{aligned} F_e(e_\alpha) = & \frac{1}{2}C_{11}(e_1 + e_2)^2 + \frac{1}{2}C_{33}e_3^2 + \frac{1}{2}C_{44}(e_4^2 + e_5^2) \\ & + \frac{1}{2}C_{66}(e_6^2 - 4e_1e_2) + C_{14}[(e_1 - e_2)e_4 + e_5e_6] \\ & + C_{13}e_3(e_1 + e_2), \end{aligned} \quad (3)$$

where $C_{\alpha\beta}$ are the elastic constants ($C_{66} = \frac{C_{11}-C_{12}}{2}$), and e_α correspond to the strain components with $\alpha, \beta = \bar{1}, \dots, 6$ being the Voigt indices [23]. Finally, the energy due to the linear-quadratic coupling terms ($e_\alpha M^2$) between the strains and the induced magnetization reduces to

$$\begin{aligned} F_c(e_\alpha, M) = & K_{11}(e_1 + e_2)M^2 + K_{31}e_3M^2 \\ & + K_{12}((e_1 - e_2) \cos 2\phi + e_6 \sin 2\phi)M^2 \\ & + K_{41}(e_4 \cos 2\phi + e_5 \sin 2\phi)M^2, \end{aligned} \quad (4)$$

where ϕ is the angle of the field with respect to the direction of propagation (the x direction, see Fig. 1) and $K_{\alpha\beta}$ are the coupling coefficients. The solutions for the strains induced by the magnetic field are determined by minimizing the total free energy with respect to the strains, $\partial F_t / \partial e_\alpha = 0$, and give

$$\begin{aligned} e_1 - e_2 = & \frac{C_{44}K_{12} - C_{14}K_{41}}{C_{14}^2 - C_{44}C_{66}}M^2 \cos 2\phi, \\ e_1 + e_2 = & \frac{C_{33}K_{11} - C_{13}K_{31}}{C_{13}^2 + C_{33}(C_{66} - C_{11})}M^2, \\ e_3 = & -\frac{C_{13}K_{11} + (C_{66} - C_{11})K_{31}}{C_{33}(C_{66} - C_{11}) + C_{13}^2}M^2 \\ e_4 = & -\frac{C_{14}K_{12} - C_{66}K_{41}}{C_{14}^2 - C_{44}C_{66}}M^2 \cos 2\phi, \\ e_5 = & -\frac{C_{14}K_{12} - C_{66}K_{41}}{C_{14}^2 - C_{44}C_{66}}M^2 \sin 2\phi, \\ e_6 = & -\frac{C_{44}K_{12} - C_{14}K_{41}}{C_{14}^2 - C_{44}C_{66}}M^2 \sin 2\phi. \end{aligned} \quad (5)$$

Based on this analysis for the paramagnetic state, the effect of a field applied along the a axis (which coincides with the direction of propagation of the acoustic mode, $\phi = 0$) is to produce lattice distortions ($e_1 - e_2$ and e_4) proportional to the square of the induced uniform magnetization. In other words, as a field along the a axis removes only the c -axis threefold symmetry, a lowering of the crystal symmetry from trigonal to monoclinic is taking place due to the magnetoelastic coupling. Moreover, as the field deviates from the a direction, additional shear deformations (e_5 and e_6) are also produced, reducing the symmetry further down to triclinic. These deformations are

therefore responsible for the angular dependence of the elastic constants relative to the field direction. The analytic solution for C_{11} is obtained using

$$C_{11}(H, \phi) = \frac{\partial^2 F_t}{\partial e_1^2} - \frac{\left(\frac{\partial^2 F_t}{\partial e_1 \partial M}\right)^2}{\frac{\partial^2 F_t}{\partial M^2}}. \quad (6)$$

Thus the influence of a field applied in the ab -plane on the relative variation on C_{11} is given by

$$\frac{\Delta C_{11}}{C_{11}}(H, \phi) = -\frac{4M^3}{HC_{11}}(K_{11} + K_{12} \cos 2\phi)^2. \quad (7)$$

As shown in Fig. 5, this analytical solution [Eq. (7)] agrees well with the experimental data obtained in the paramagnetic state. We obtain that the coupling constants are $K_{11} = 0.00234(2) \text{ T}^2 \text{ m}^3 \text{ J}^{-1}$ and $K_{12} = 0.000217(2) \text{ T}^2 \text{ m}^3 \text{ J}^{-1}$, which lead to magnetostriction deformations [Eqs. (5)] of about

$$\begin{aligned} e_1 - e_2 = & 1.62(2) \times 10^{-6} \text{ at } H = 16 \text{ T}, \\ e_1 + e_2 = & 6.20(6) \times 10^{-6} \text{ at } H = 16 \text{ T}. \end{aligned}$$

In order to quantify these constants, we consider that $C_{14} = C_{13} = 0$ as they are, in general, significantly smaller than the principal elastic constants C_{ji} . These numerical estimates indicate that the spin-lattice coupling is effectively weak and therefore, any structural transitions associated with the chiral state are likely to be of the same order of magnitude. This is also compatible with the fact that no significant steplike variation in $\Delta C_{11}/C_{11}$ is observed at T_N (Fig. 3).

The angular dependence in the paramagnetic state (30 K at 16 T) is also compared in Fig. 6(b) to similar results obtained in the chiral magnetic state (20, 10, and 2.5 K). In the ordered state, we should expect deviations from the angular dependence associated with the uniform magnetization [Eq. (7)] due to the antiferromagnetic chiral order and the field induced electric polarization. While the angular dependence due to the uniform magnetization is maintained at all temperatures, the evidence of a steplike feature with an angular hysteresis (between clockwise and counterclockwise measurements) around -12° is observed only in the magnetically ordered state. Moreover, measurements at $T = 2.5$ K [see Fig. 6(a)] also indicate that the width of the angular hysteresis increases as the field increases. The variation of $\Delta C_{11}/C_{11} \sim 3.2 \times 10^{-5}$ measured at 2.5 K and 16 T, clearly indicates the existence of a small coupling between the strains, the chiral magnetic state, and the field induced polarization. We attribute the hysteresis to a first order transition associated with the sudden change in the field-induced distortion of the chiral magnetic state, which affects the direction of the electric polarization via the magnetoelectric coupling. As shown by Lee *et al.* [11], a magnetic field H_a induces a polarization P_{b^*} (normal to the field) while the field H_{b^*} rather stabilizes a polarization along the a axis (P_a). Therefore we can assume that the polarization induced along b^* when the field is oriented along a ($\phi = 0$) will suddenly rotate by 90° toward the a axis when the field rotates by more than 12° toward the b^* axis ($\phi = 90^\circ$), in an attempt to maintain an angle of $\approx 90^\circ$ between the applied magnetic field and the polarization. While at this point we can only

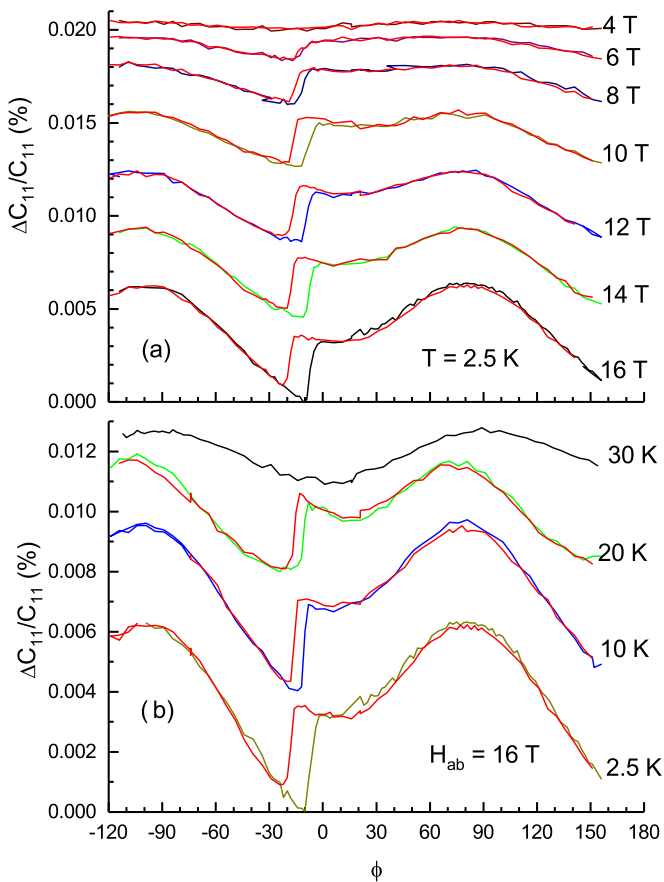


FIG. 6. Angular dependence of $\Delta C_{11}/C_{11}$ measured as a function of a constant field rotating in the ab plane (a) for different field values at $T = 2.5$ K and (b) for different temperatures at $H = 16$ T. For clarity, each curve has been shifted vertically with respect to each other. The two curves showing a hysteresis correspond to a clockwise and anticlockwise rotation of the magnetic field.

speculate about the polarization direction, our measurements demonstrate that the change in the polarization direction, associated with the magnetic chiral state, is not continuous as the field is rotated in the ab plane.

In summary, our study of the elastic properties of $\text{Ba}_3\text{NbFe}_3\text{Si}_2\text{O}_{14}$ reveals no structural transition at 120 K as proposed by Toulouse *et al.* [16], while the magnetic

phase transition associated with the chiral state is clearly visible at $T_N = 27.1(1)$ K (Fig. 3). According to the electric polarization data of Lee *et al.* [11], this magnetic transition is accompanied by a spontaneous ferroelectric polarization with a dominant component along the a axis at zero magnetic field. In that case, based on symmetry arguments, the presence of a electric polarization along the a axis should reduce the crystal symmetry. However, so far, only indirect indications of such a structural transition have been obtained from resonant x-ray diffraction [29,30] and from Mössbauer measurements [31]. Those were modeled with two inequivalent sites per trimer which lead to inequivalent intratriangle J_1 interactions. In that context, the spin configuration deviates from the 120° arrangement, as recently confirmed by Neutron scattering [13]. Moreover, due to the helical nature of the spin arrangement along the c axis over seven planes, Chaix *et al.* [13] proposed a “bunched helical structure” in order to account for a net electric polarization over the period of the helix. Independently of the mechanisms that lead to the observation of an electric polarization at zero field, the presence of a net polarization should coincide with structural deformations. Assuming that the variation in C_{11} is due to the lattice-polarization coupling, the observation of an angular hysteresis in the chiral magnetic state gives additional evidence for a symmetry breaking in the magnetic chiral state associated with the field-induced polarization [11].

In conclusion, as the estimated deformation amplitude is small ($e_1 - e_2 \leq 10^{-5}$), this might explain why there is no direct observation based on thermal expansion or x-ray measurements. While $\text{Ba}_3\text{NbFe}_3\text{Si}_2\text{O}_{14}$ should still be considered to be a magnetically induced multiferroic, the microscopic mechanism leading to the magnetoelectric effect in zero field remains unclear. However, the polarization enhancement under a magnetic field can be accounted for by the field-induced deformation of the 120° magnetic arrangement based on the magnetoelectric coupling form, based purely on symmetry arguments [13].

ACKNOWLEDGMENTS

The authors wishes to thank M. Castonguay for very valuable technical support. This work was supported by the Natural Sciences and Engineering Research Council of Canada (NSERC) and the Fonds de recherche du Québec - Nature et technologies (FRQNT).

- [1] T. Kimura, J. C. Lashley, and A. P. Ramirez, *Phys. Rev. B* **73**, 220401 (2006).
- [2] H. Mitamura, S. Mitsuda, S. Kanetsuki, H. A. Katori, T. Sakakibara, and K. Kindo, *J. Phys.: Conf. Ser.* **51**, 557 (2006).
- [3] M. Kenzelmann, G. Lawes, A. B. Harris, G. Gasparovic, C. Broholm, A. P. Ramirez, G. A. Jorge, M. Jaime, S. Park, Q. Huang *et al.*, *Phys. Rev. Lett.* **98**, 267205 (2007).
- [4] K. Kimura, H. Nakamura, S. Kimura, M. Hagiwara, and T. Kimura, *Phys. Rev. Lett.* **103**, 107201 (2009).
- [5] H. Mitamura, R. Watanuki, K. Kaneko, N. Onozaki, Y. Amou, S. Kittaka, R. Kobayashi, Y. Shimura, I. Yamamoto, K. Suzuki *et al.*, *Phys. Rev. Lett.* **113**, 147202 (2014).
- [6] K. Cao, R. D. Johnson, F. Giustino, P. G. Radaelli, G.-C. Guo, and L. He, *Phys. Rev. B* **90**, 024402 (2014).
- [7] L. N. Bulaevskii, C. D. Batista, M. V. Mostovoy, and D. I. Khomskii, *Phys. Rev. B* **78**, 024402 (2008).
- [8] D. I. Khomskii, *J. Phys.: Condens. Matter* **22**, 164209 (2010).
- [9] V. Simonet, M. Loire, and R. Ballou, *Eur. Phys. J.: Spec. Top.* **213**, 5 (2012).
- [10] K. Marty, V. Simonet, E. Ressouche, R. Ballou, P. Lejay, and P. Bordet, *Phys. Rev. Lett.* **101**, 247201 (2008).
- [11] N. Lee, Y. J. Choi, and S.-W. Cheong, *Appl. Phys. Lett.* **104**, 072904 (2014).

- [12] H. D. Zhou, Y. Barlas, C. R. Wiebe, Y. Qiu, J. R. D. Copley, and J. S. Gardner, *Phys. Rev. B* **82**, 132408 (2010).
- [13] L. Chaix, R. Ballou, A. Cano, S. Petit, S. de Brion, J. Ollivier, L.-P. Regnault, E. Ressouche, E. Constable, C. V. Colin *et al.*, *Phys. Rev. B* **93**, 214419 (2016).
- [14] D. I. Khomskii, [arXiv:1510.05174](https://arxiv.org/abs/1510.05174).
- [15] M. Loire, V. Simonet, S. Petit, K. Marty, P. Bordet, P. Lejay, J. Ollivier, M. Enderle, P. Steffens, E. Ressouche *et al.*, *Phys. Rev. Lett.* **106**, 207201 (2011).
- [16] C. Toulouse, M. Cazayous, S. de Brion, F. Levy-Bertrand, H. Barkaoui, P. Lejay, L. Chaix, M. B. Lepetit, J. B. Brubach, and P. Roy, *Phys. Rev. B* **92**, 104302 (2015).
- [17] P. Bordet, I. Gelard, K. Marty, A. Ibanez, J. Robert, V. Simonet, B. Canals, R. Ballou, and P. Lejay, *J. Phys.: Condens. Matter* **18**, 5147 (2006).
- [18] G. Quirion, M. Lapointe-Major, M. Poirier, J. A. Quilliam, Z. L. Dun, and H. D. Zhou, *Phys. Rev. B* **92**, 014414 (2015).
- [19] G. Quirion, M. L. Plumer, O. A. Petrenko, G. Balakrishnan, and C. Proust, *Phys. Rev. B* **80**, 064420 (2009).
- [20] G. Quirion, W. Wu, O. Aktas, J. Rideout, M. J. Clouter, and B. Mróz, *J. Phys.: Condens. Matter* **21**, 455901 (2009).
- [21] G. Quirion, X. Han, M. L. Plumer, and M. Poirier, *Phys. Rev. Lett.* **97**, 077202 (2006).
- [22] G. Quirion, M. Abu-Kharma, I. A. Sergienko, M. Bromberek, M. Clouter, and B. Mroz, *J. Phys.: Condens. Matter* **15**, 4979 (2003).
- [23] E. Dieulesaint and D. Royer, *Elastic Waves in Solids* (Wiley, 1980).
- [24] K. Marty, P. Bordet, V. Simonet, M. Loire, R. Ballou, C. Darie, J. Kljun, P. Bonville, O. Isnard, P. Lejay *et al.*, *Phys. Rev. B* **81**, 054416 (2010).
- [25] C. Stock, L. C. Chapon, A. Schneidewind, Y. Su, P. G. Radaelli, D. F. McMorrow, A. Bombardi, N. Lee, and S.-W. Cheong, *Phys. Rev. B* **83**, 104426 (2011).
- [26] G. Quirion, T. Taylor, and M. Poirier, *Phys. Rev. B* **72**, 094403 (2005).
- [27] K. Y. Choi, Z. Wang, A. Ozarowski, J. van Tol, H. D. Zhou, C. R. Wiebe, Y. Skourski, and N. S. Dalal, *J. Phys.: Condens. Matter* **24**, 246001 (2012).
- [28] H. D. Zhou, L. L. Lumata, P. L. Kuhns, A. P. Reyes, E. S. Choi, N. S. Dalal, J. Lu, Y. J. Jo, L. Balicas, J. S. Brooks *et al.*, *Chem. Mater.* **21**, 156 (2009).
- [29] V. Scagnoli, S. W. Huang, M. Garganourakis, R. A. de Souza, U. Staub, V. Simonet, P. Lejay, and R. Ballou, *Phys. Rev. B* **88**, 104417 (2013).
- [30] M. Ramakrishnan, Y. Joly, Y. W. Windsor, L. Rettig, A. Alberca, E. M. Bothschafter, P. Lejay, R. Ballou, V. Simonet, V. Scagnoli *et al.*, *Phys. Rev. B* **95**, 205145 (2017).
- [31] I. S. Lyubutin, P. G. Naumov, B. V. Mill', K. V. Frolov, and E. I. Demikhov, *Phys. Rev. B* **84**, 214425 (2011).